



Preparation, characterization and cell performance of durable nafion/SiO₂ hybrid membrane for high-temperature polymeric fuel cells

M. Amjadi^a, S. Rowshanzamir^{a,b,*}, S.J. Peighambaroust^a, S. Sedghi^b

^a School of Chemical Engineering, Iran University of Science and Technology, Narmak, Tehran 16846-13114, Iran

^b Fuel Cell Laboratory, Green Research Center, Iran University of Science and Technology, Narmak, Tehran, Iran

ARTICLE INFO

Article history:

Received 17 December 2011

Received in revised form 5 February 2012

Accepted 7 March 2012

Available online 2 April 2012

Keywords:

Proton exchange membrane fuel cell

Nafion

Leaching

Hydrogen crossover

Water uptake

Sol-gel

ABSTRACT

The Nafion 117 membrane has doped with SiO₂ particles by in situ sol-gel reaction. In order to minimize leaching of doped particles, the reaction conditions are optimized using full factorial design of experiment. The results obtained from the full factorial analysis indicate that the minimum amount of leaching takes place at 60 °C, without addition of acid, and with the swelling of membranes prior to the reaction. The membranes, prepared at optimum reaction conditions, are characterized for water uptake, thermal stability, proton conductivity, and cell performance. Furthermore, Nafion/SiO₂ composites are investigated to reduce the hydrogen permeation rate across the membrane. The Nafion/SiO₂ composites demonstrate significantly low hydrogen permeability. Moreover, the water uptake of Nafion/SiO₂ membrane with 7% of doping level increase up to 43% that is 30% higher than that of the pure Nafion membrane. DSC Measurements for modified samples show an increase in T_g as compared to unmodified sample. In general, the proton conductivities of hybridized membranes under ambient temperature are lower than that of the pure membrane. However, at 110 °C and in low humid conditions, the modified membranes show increased fuel cell performance than the pure Nafion. Among the composite membranes, the sample with 5–7% of SiO₂ content exhibits higher water uptake and better performance of fuel cell test.

© 2012 Elsevier B.V. All rights reserved.

1. Introduction

Proton exchange membrane fuel cells (PEMFCs) are in the forefront among other fuel cell technologies, and significant efforts in the fundamental areas of research have enabled rapid advances in the PEMFC technology development [1,2]. PEMFCs provide the highest power density and specific power among all the other fuel cell types and hence have applications in portable devices, transportation, and stationary power generation [3,4]. Common PEM fuel cells operate in the temperature range between 60 °C and 80 °C, while elevating the operating temperature provides improved carbon monoxide tolerance, faster electrode kinetics and simpler thermal management [5–7]. Polymeric membrane electrolyte is a vital part of the PEM fuel cell. In general, the membrane serves the purposes of: (1) a barrier between the anode and cathode reactants, (2) proton conduction, and (3) electronic insulator. Increasing the operation temperature of PEM fuel cell results in

the dehydration of the polymer electrolyte, leading to increased membrane resistance and degradation of the membrane-electrode interface. A perfluorosulfonic acid (PFSA) based membranes, such as the Nafion, is commonly employed as the electrolyte for PEM fuel cells because of its excellent chemical, mechanical, and thermal stability, as well as its relatively high proton conductivity when fully hydrated [8–11]. However, Nafion has certain disadvantages for PEM fuel cell applications. The proton conductivity of a Nafion membrane depends strongly upon the relative humidity (RH) of the reactant gases and the membrane needs to be kept humidified for good ionic conductivity [10–12]. In addition, the mechanical and dimensional stability of the polymeric chain of Nafion can be diminished at high temperatures as a result of its relatively low glass transition temperature [9]. Besides, according to analytical reports, gas crossover of Nafion increases with temperature rises [13]. Thus, one of the major challenges in the current PEM fuel cell research is to develop an upgraded membrane with the ability of working under elevated temperatures and low humidification of reactant gases. As a possible approach to overcome the temperature limitation, alternative polymeric electrolytes, such as polybenzimidazole (PBI), have been intensively investigated [3]. However, an effective alternative material has not been yet found to replace Nafion as the standard electrolyte of PEMFC.

* Corresponding author at: Tehran – Resalat Sq., Hengam St., Elmosanat Av., Iran University of Science & Technology, Green Research Centre, Postal Code: 16846-13114, Iran. Tel.: +98 2177491223; fax: +98 2177491242.

E-mail address: rowshanzamir@iust.ac.ir (S. Rowshanzamir).

In this context, significant efforts have been made to modify Nafion membranes for the application at low humidity or high temperatures [14–18]. One of the effective approaches is to incorporate hygroscopic metal oxide particles such as silica, zirconia, titania, and zirconium phosphate into the hydrophilic domains of the polymer electrolyte membrane to enhance the water retention of the Nafion as well as membrane stability at high temperature applications [19–23]. Furthermore, fuel crossover can be reduced if inorganic particles are placed along gas diffusion pathways, i.e., within the polar clusters [24].

Nafion metal oxide hybrid membrane may be produced either by physical mixing of oxide powder with Nafion solution, or by the sol-gel reactions. The doping methods not only have significant effects on Nafion physical characteristics, but also improve stability of doped particles in the membrane. Our previous work [25] shows that physical mixing produces larger particles with less uniform distribution compared to the sol-gel method.

In the case of in situ sol-gel derived Nafion/metal oxide composite membranes, samples were soaked in a bath containing alkoxide of metal-ex, tetrabutylortitanate (TBT) to produce TiO_2 or tetraethylorthosilicate (TEOS) for SiO_2 particles-allowing the hydrolyzed alkoxide molecules to permeate and diffuse into the organic phase. The polar molecules would preferentially migrate to the hydrophilic polar clusters inside the membrane. In fact, in situ sol-gel technique is a site-targeted synthesis of such inorganic oxide inclusions as quasi-networks in the hydrophilic domains.

Studies on Nafion/metal oxide composite membranes have attracted the attention of many research groups. Santiago et al. [26] incorporated TiO_2 into Nafion by sol-gel method to form a composite membrane that shows improved cell performance at 130 °C. However, no morphological study has been reported in their work. Daiko et al. [27] synthesized Nafion composite membrane with combination of both TEOS and TBT alkoxides and tested them in direct methanol fuel cell. They concluded that infiltrated oxides improve the membrane barrier property against methanol.

Jiang et al. [28] reported the inorganic modification of Nafion using tetraethylorthosilicate (TEOS) by solution casting method. They demonstrated an increase in fuel cell performance at low loadings (5 wt.%). However, the performance decreased with an increase in inorganic content. Malhotra and Datta [29] showed that incorporation of inorganic solid acids (phosphotungstic acid) in Nafion resulted in improved water retention capacity due to additional acidic sites and hence led to high fuel cell performance at elevated temperatures. However, higher water solubility of the incorporated inorganic acids resulted in excessive swelling leading to membrane failure.

In application of doped membranes in real PEM, stability of inorganic dopants is a vital issue, but only a few reports are available that consider leaching of doped particles through the composite membrane. Mauritz et al. claimed that the $\text{SiO}_2 \cdot \text{OH}_x$ in-growth cannot be leached out of the membrane. They did not set stability of silica particles against the acid treatment step as they were not supposed to apply these membranes for real PEM cell [30,31]. Miyake et al. used SiO_2 -dispersed (3–26 wt.%) Nafion for a PEFC, but they just washed the membranes in boiled water [32]. Jung et al. also used SiO_2 -dispersed (6.4–21 wt.%) Nafion for a direct methanol fuel cell (DMFC), but the treatment procedure was not described [33]. Hagihara et al. reported reaction time and reaction temperature effects on leaching amount of doped inorganics, but they did not apply a design of experiment (DOE) for their investigations [34].

In this work, Nafion/ SiO_2 composite membranes were produced in the different doping levels of SiO_2 particles by in situ sol-gel synthesis of silica particles in preformed Nafion membranes. Since stability of doped particles in real cell application is of great importance, for minimizing the leaching of particles, the sol-gel reaction conditions were optimized by using full factorial design of

Table 1
Control factors and there levels.

Factor	Level 1	Level 2
Reaction temperature	60 °C	Ambient temperature
pH adjustment	With acid addition (pH = 2.3)	Without acid addition
Swelling in methanol prior the reaction	Yes (methanol:water, 2:1)	No

experiment. The membranes have been characterized by thermal stability, water uptake, proton conductivity, and cell performance. Also, as a novel research, we compared hydrogen permeability of Nafion/ SiO_2 composite membrane and a bear one.

2. Experimental

2.1. Chemicals and materials

Nafion 117 membranes and Nafion solution (5 wt.%) were purchased from Electrochem. Tetraethylorthosilicate (TEOS) 98%, sulfuric acid (H_2SO_4) 98%, hydrogen peroxide (H_2O_2) 30%, and all other chemicals obtained from Merck and used as received. The water used in all experiments was prepared in a Millipore Milli-Q system.

2.2. Samples preparation

The commercial Nafion 117 membranes of 2.5 cm × 2.5 cm were first cleaned in 3% H_2O_2 at 80 °C for 1 h. They were then rinsed with deionized water and subsequently treated in 1 M H_2SO_4 for 1 h at 80 °C. Finally, these membranes were rinsed in deionized water at 80 °C for several times. After drying at room temperature under vacuum, the purified Nafion membranes were dipped in precursor solution to accomplish the hydrolysis in the membranes during the treatment. Precursor solutions were prepared by mixing TEOS and methanol with the ratio of 3:2 (vol.%). Different reaction times lead to different loading levels of doped particles.

After the infiltration time, membrane surfaces were rinsed several times with methanol to wash any silica layer which might be deposited on the membrane surface. Finally, the membranes were dried at 70 °C under vacuum for 12 h to form condensed silicon oxide network within the membrane. The weight percent of doped particles is calculated with dry weight of membranes before and after reaction.

In order to achieve the optimum status of the reaction conditions, leading to the creation of more stable particles in the membrane, three main factors, including temperature, pH, and methanol content, is studied using full factorial experimental design. Each of these factors is considered at two levels. Therefore, eight different experiments will be set up according to 2^3 full factorial design. Table 1 represents these factors and their levels of study in this experimental design. Temperature has two levels; 60 °C, known as the level 1, and ambient temperature, known as level 2. For pH parameter, addition of acid to the solution is indicator of level 1. In contrast, its second level is specified by the lack of acid in the solution. Moreover, content of methanol as the swelling agent is the third parameter of this experimental design. First and second levels of this parameter are determined by methanol existence and absence in the solution, respectively. The full factorial design of experiments for three parameters and each at two levels is listed in Table 2. Reaction time for all of the samples tested in this design is considered equal. For activating $-\text{SO}_3\text{H}$ groups of the membrane clusters and estimating the leaching level of the doped particles, the samples are rinsed in the sulfuric acid solution for 1 h. Then, these samples are washed in boiling water to remove excess

Table 2
Experimental sets from 2ⁿ full factorial design (coded form).

Samples	Reaction temperature level	pH level	Swelling level
A1	1	1	1
A2	1	1	2
A3	1	2	1
A4	1	2	2
A5	2	1	1
A6	2	1	2
A7	2	2	1
A8	2	2	2

acid. Leaching level of the particles is determined using the weight difference before and after the final processing step.

2.3. Membrane characterization

Water uptake was calculated with the weight difference of wet and dry samples of a composite membrane. To obtain the wet weight, a membrane sample was equilibrated with distilled water at room temperature or 80 °C overnight. The wet sample was then removed, dried with tissue papers, and then weighed. The dry weight was also measured after vacuum drying of the sample at 100 °C for 1 day. The water uptake was calculated using the weights of wet membrane (W_w) and dry membrane (W_d) with following equation:

$$\text{water uptake(\%)} = \frac{(W_w - W_d)}{W_d} \times 100 \quad (1)$$

To obtain the glass transition temperature (T_g) of samples, differential scanning calorimetry (DSC) was performed on a Netzsch DSC-Maia-200F3. The runs were performed at heating rate of 20 °C min⁻¹ in nitrogen atmosphere with flow rate of 50 ml min⁻¹. Before each run, the sample was dried at 80 °C for 8 h to suppress the endothermic peak by water desorption during the measurement. The proton conductivity of membranes was measured by the two electrode AC impedance method [35]. A sample of the membrane was placed between two gold disc electrodes and tested in the potentiostatic mode. The measurements were carried out on the potentiostat/galvanostat (PARSTAT 2263) provided by Princeton Applied Research. The spectra were recorded between 100 kHz and 100 Hz with 12 points per decade and maximum perturbation amplitude of 10 mV. The Z. Sim software was used to analyze the data. All the samples were submerged in water overnight prior to test. The proton conductivity of membranes (σ) was calculated from impedance data using the Eq. (2):

$$\sigma = \frac{L}{RS} \quad (2)$$

where L and S are the thickness and area of the membrane, respectively. Also, R is the resistance of the membrane obtained from the low intersect of the Nyquist plot with the Re (z) axis. Note that dimensions of the membranes have been measured after hydration step.

2.4. Hydrogen crossover measurement

Pure gas crossover measurements were carried out for H₂ using a constant pressure/variable volume method at room temperature. An experimental apparatus according to the ASTM D1434 was designed for gas permeation measurements. The rate of the crossing over stream was measured using a flow meter. The feed pressure for all of the permeation measurements was set

to 2.5 bars. By measuring the flow rate of the permeated stream, permeance of the passed gas can be calculated using Eq. (3).

$$K = \frac{J}{A\Delta p} \quad (3)$$

A , Δp , and J are effective membrane area, pressure drop, and the permeated gas flow rate, respectively. At steady state condition, Eq. (4) is used for calculating gas permeance in term of barrer cm⁻¹.

$$Q = \frac{P}{L} = 10^{10} \frac{A' T_{STP}}{600 A T \Delta p} \left(\frac{dH}{dt} \right) \quad (4)$$

P , L , (dH/dt) and A' are the gas permeability, thickness of the membrane, constant downstream flow rate, and the cross-section area of the manometer tube, respectively. T_{STP} is used to convert the flow rate of the permeated gas to standard condition. 600 and 10¹⁰ are conversion factors.

2.5. Membrane electrode assembly (MEA) preparation

Three different membrane electrode assemblies were made with pure Nafion 117 (PN), with Nafion/SiO₂ hybrid membrane including 2 wt.% of SiO₂ (NS.1), and with Nafion/SiO₂ hybrid membrane including 7 wt.% of SiO₂ (NS.2). In order to fabricate MEAs, the membranes were cleaned and treated to ensure that they are completely in the protonic form. The treatment procedure is reported elsewhere [35]. Membranes were hot pressed between two electrodes to form the membrane-electrode assemblies. In order to prepare the electrodes, Pt catalyst (Pt/C, 20%, Ruth) was mechanically mixed for 30 min in isopropanol with the loading of 0.4 mg cm⁻² for both anodic and cathodic sites. Subsequently, a 30 wt.% of PTFE (ElectroChem, EC-TFE 30) solution was added to the mixture and stirred by ultrasound (Sounopuls, HD2200). This slurry was coated on the Toray carbon paper (ElectroChem, Teflon treated, EC-TP1-060T) by spraying apparatus. Then, the sample was dried for 24 h in air and then for 60 min in an inert gas (nitrogen 99.99%) at 225 °C. Then, the dried electrodes were pressed by a rolling apparatus and sintered for 30 min in an inert gas (nitrogen 99.99%) at 350 °C. Electrodes were impregnated by brushing a 5% Nafion solution (ElectroChem, EC-NS-05) with loading of 2 mg cm⁻² onto the electrocatalyst layer. The electrodes were dried in oven for 60 min at 80 °C. The membrane was hot-pressed between two electrodes at 140 °C for 2 min and 120 atm to complete MEA.

2.6. Fuel cell performance

A schematic diagram of the experimental apparatus employed in this study is shown in Fig. 1. Pure hydrogen and oxygen were used as the fuel and oxidant gases, respectively. Humidification of the reactants was achieved by temperature-controlled water bottles. The temperature of bottles could be calibrated to yield the different relative humidity (RH) values and dew points. Flow rates of fuel and oxidant gases are controlled using the mass flow controller (MFC, AALBORG, GFC171). The PEM fuel cell was pressurized by a backpressure regulator to the desired pressure condition. A single PEM fuel cell (ElectroChem, FC05-01SP) with active surface area of 5 cm² was used for all experiments in this study. The temperature of cell was controlled via a temperature controller (Barnant Company, 8900-15). The gas connections between the gas control system and the fuel cell inlets are well insulated to prevent cooling and condensing of the water vapor on the path to the fuel cell. Cell voltage and current were determined simultaneously at different loads using a Multimeter, and the polarization curves (voltage versus current density) of the PEMFC were obtained.

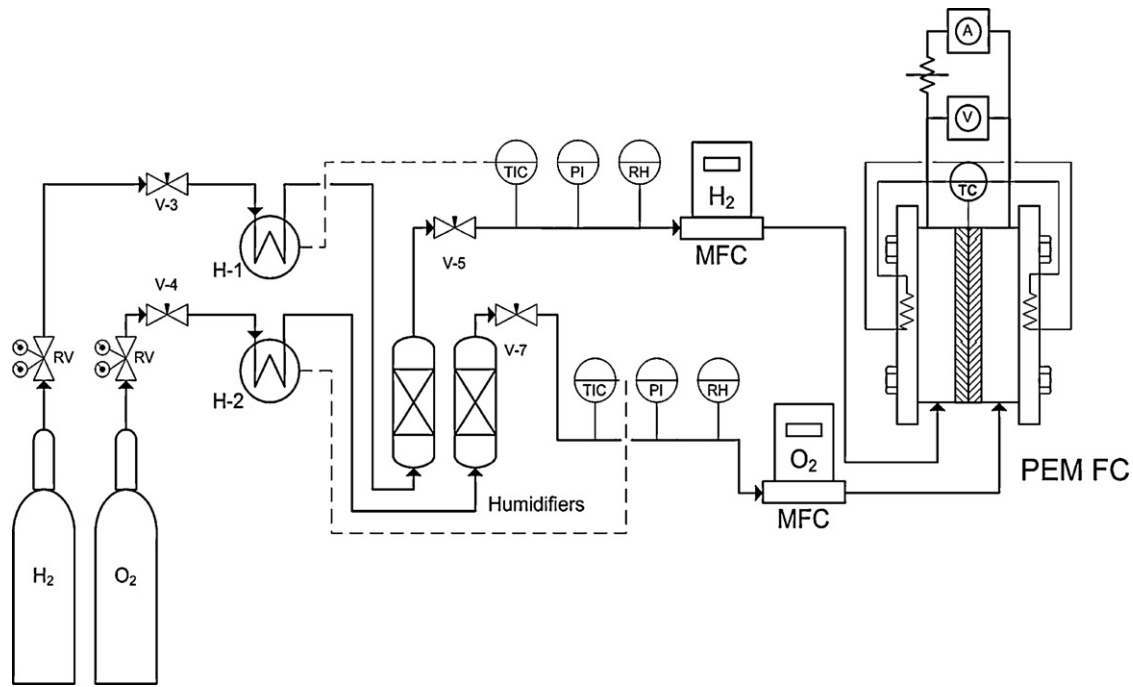


Fig. 1. Flow diagram of the experimental set up.

3. Results and discussion

3.1. Optimum conditions of the sol–gel reaction

After the final treatment step, usually a major percentage of the doped metal oxides are dissolved in the solution. Most of the researchers have ignored the studies of the final processing step or even have not done this step at all. But, in view of the fact that the membrane is always exposed to water in the real fuel cell applications, the stability of the doped particles is important.

Table 3 represents the impact of hydrolysis conditions on the remaining amount of SiO₂ particles. After the final treatment step, membranes are put again in the vacuum oven to determine the dissolution amount of the metal oxide. Leaching percentage and dissolution amount of the mineral particles are calculated using the weight losses of the membranes. According to the results of Table 3, optimum conditions of the hydrolysis reaction, resulting in the minimum leaching level of the doped particles, is achieved at 60 °C, without addition of acid, and in the presence of methanol as swelling agent. This situation is related to the A3 sample. Therefore, all other samples are prepared with A3 conditions for specification tests.

Positioning of mineral particles in the interspaces between acidic Nafion clusters has reduced severely the possibility of their

leaching. Since methanol is a good solvent for the Nafion membrane, it seems that immersion of membranes in the methanol before sol–gel reaction, leads to their swelling and facilitates the accessibility of precursor solution to the reaction sites. Moreover, higher temperature (such as 60 °C) leads to more swelling of the membranes and eases the particle penetration into ionic clusters.

Furthermore, acidic environment causes a quick reaction. Hence, it is very effective in increasing doping level before final treatment. Yet, higher reaction rate, caused by acidic environment, leads to the occurrence of hydrolysis reaction and generation of particles outside Nafion clusters. Thus, they will be easily leached in the final treatment step.

Leaching data were analyzed by Minitab Software to determine importance of each parameter. Fig. 2 represents the main effects of each factor on leaching amount of doped particles. The data presented in Fig. 2 are the mean values at each level for the leaching percentage. Each small box has two means connected by a solid line. The sharper the gradient of the line, the larger the difference between the two means and therefore the greater the influence of the factor on the leaching amount. As seen in the Fig. 2, based on lines' slopes, the most important factor influencing leaching is swelling. This indicates the importance of Nafion network accessibility for mineral particles to be reinforced in.

After determining the optimum reaction conditions by experimental design, several samples with different doping levels are prepared at optimum condition for investigating the effects of addition of SiO₂ particles on the Nafion membrane characteristics. The specifications of these final samples are presented in Table 4.

For more details, the doping amounts of samples are plotted as a function of reaction time in Fig. 3. As seen in this figure, the weight increases with increasing reaction time and reaches to an almost constant level after a long period of time. Also in Fig. 3, the weight change is re-plotted as a function of the square root of reaction time. Note that the linearity suggests that the reaction is controlled by diffusion process. This result has also been confirmed by Daiko et al. [36].

Since the diffusion process is controlling the sol–gel reaction, the swelling of membranes in methanol solution before reaction

Table 3
Leaching amount of SiO₂ after final treatment.

Samples	Doping levels: before final treatment (wt.%)	Doping levels: after final treatment (wt.%)	Leaching amount (%)
A1	10.7	8.6	20.0
A2	9.1	6.4	29.2
A3	8.9	8.4	5.1
A4	8.5	6.7	21.0
A5	9.0	7.4	17.7
A6	8.6	5.8	33.0
A7	8.7	6.6	21.5
A8	8.5	5.8	32.0

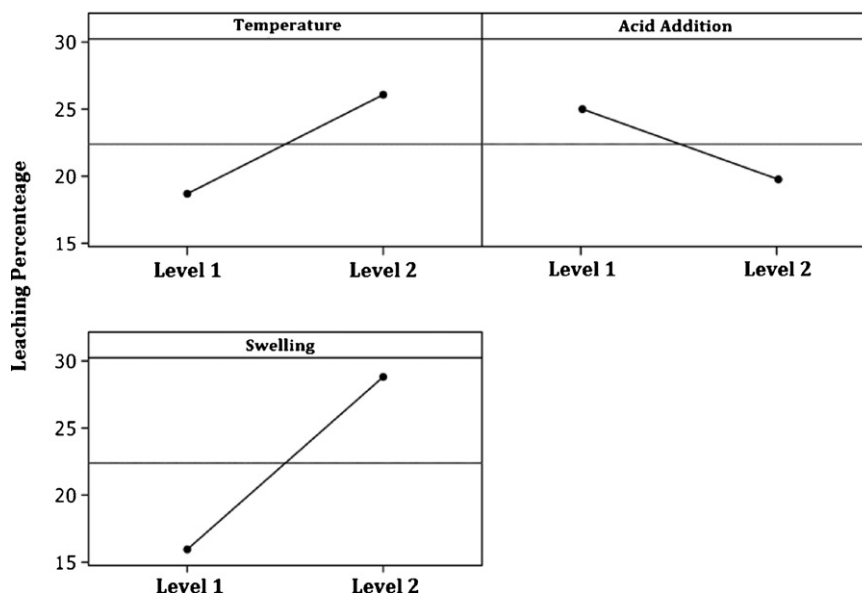
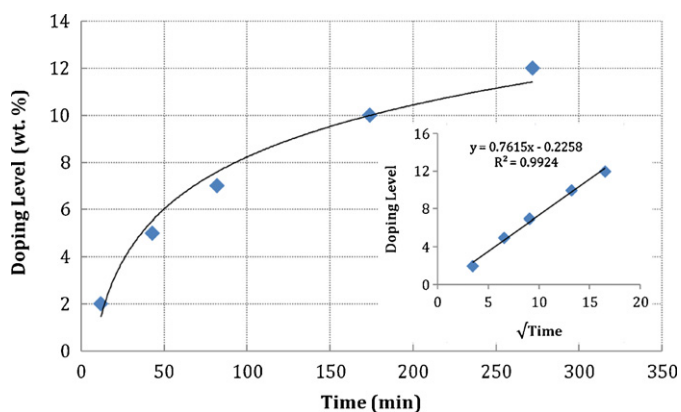


Fig. 2. Main effects plot for leaching amount.

Fig. 3. Doping amount of SiO₂ particles versus infiltration time.

could facilitate the diffusion of TEOS monomers into Nafion clusters resulting in stable particles which would not leach easily. This consequence is in agreement with leaching study results indicating that swelling of samples is the most important parameter affecting particles leaching.

3.2. Water uptake

Fig. 4 shows the water uptake results of pure Nafion and Nafion/SiO₂ composite membranes at two different hydration temperatures. At 80 °C, all the samples show higher water uptake in comparison to the ambient temperature. These results are in agreement with published data from various researchers. Jalani et al.

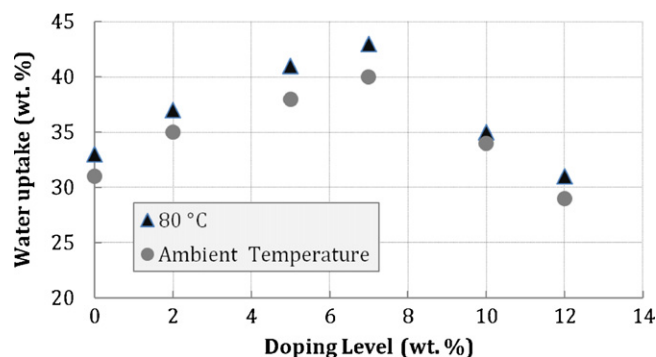


Fig. 4. Water uptake of composite membranes in two different temperatures.

[37] have been found that the water sorption of Nafion membranes increases with temperature from 30 °C to 90 °C. Their sorption data also was in agreement with water sorption model which was developed by them [38,39].

In an early study, it was found that Nafion membrane becomes rubbery when the sorption temperature increases with a tendency to uptake more water [40]. This behavior i.e. more water uptake at higher temperature, is explained by the increase in the flexibility of polymer chains via a decrease in Young's Modulus (E) of membrane with temperature. Kawano et al. [41] have studied the stress–strain characteristics of Nafion membrane at different temperatures and found that the initial slope of the curves i.e., the Young's modulus (E) decreases with increasing temperature, thus softening the membrane and allowing higher water uptake. A lower Young's modulus (E) reduces the swelling pressure on the imbibed liquid thus caused

Table 4
Specifications of prepared Nafion/SiO₂ hybrid membranes.

Sample code	Reaction time (min)	Doping level (wt.%)	T_g (°C)	Thickness (μm)	Proton conductivity ($10^{-3} \text{ S cm}^{-1}$)	Transparency
PN	0	0	99	180	11.21	Completely Transparent
NS.1	15	2	–	190	7.11	Transparent
NS.2	45	5	113	190	4.34	Transparent
NS.3	80	7	118	195	3.00	Partially transparent
NS.4	175	10	125	197	0.78	Opaque
NS.5	270	12	–	–	–	Opaque

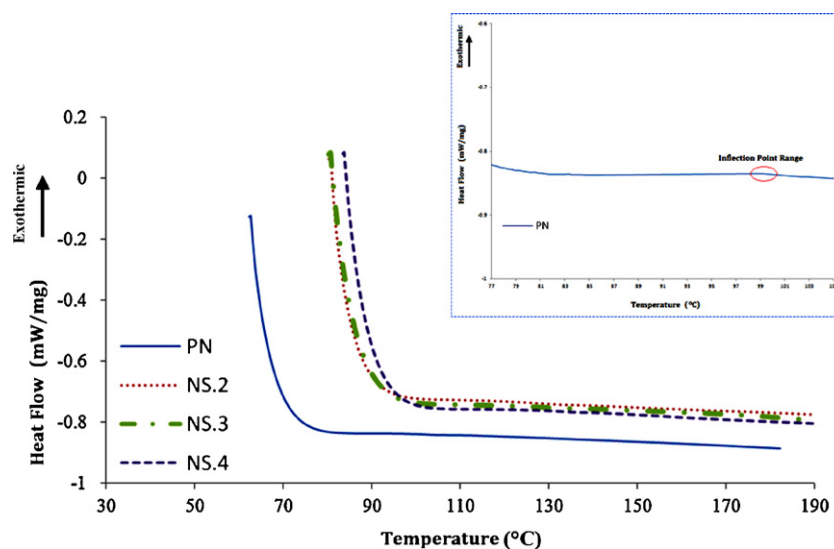


Fig. 5. DSC curves of membranes.

to equilibrate at higher sorption amount. As seen in Fig. 3, water uptake increases with an increase of SiO₂ doping level up to 7 wt.%. Water uptake of Nafion/SiO₂ membrane with 7 wt.% of doping level is 36% higher than that of the pure Nafion membrane. This can be attributed to the presence of hydrophilic inorganic particles reinforced in Nafion matrix. Because of the masking of hydrophilic HSO₃ groups in the Nafion clusters, further increase in doping amount leads to the decrease in water uptake.

3.3. DSC measurements

One of the most important characteristics of proton exchange membranes which must be improved for high temperature applications is glass transition temperature (T_g). Above this temperature, membrane loses its rigidity, and the performance of membrane decreases dramatically due to the shrinkage. Thus, PEM fuel cells must be applied below this temperature [25]. Fig. 5 shows the DSC curves for pure Nafion and Nafion/SiO₂ with 5, 7, and 10 wt.% of silica which are named as (PN), (NS.2), (NS.3), and (NS.4), respectively. The range of T_g is calculated automatically by measurement device (Netzsch), so it is not necessary to obtain T_g from inflection of curves. The results of DSC measurements are listed in Table 4. It can be seen that T_g of the composite membranes shift to the higher temperatures. As seen in Table 4, T_g increases with increasing the amount of doping level. From the DSC data, it is found that glass transition temperature of NS.2 composite membrane is 14 °C higher than that of pure Nafion membrane. This temperature difference is 19 °C and 26 °C for NS.3 and NS.4 samples, respectively. This increase of T_g reveals improved thermal stability of the Nafion/SiO₂ samples and hence provides their potential advantages for PEM fuel cell operation at high temperatures.

Such increase of T_g can be related to the free volume theory [42]. Based on this theory, thermal expansion of free volumes, the space that is not occupied by polymer chains, occurs above glass transition temperature, and polymer chains begin to fill the free volumes as a result of their enhanced thermally motivated segmental motions. Incorporation of SiO₂ particles into the Nafion polymer matrix would fill these free volumes and would cause need to more energy for starting segmental motions, which would result in higher glass transition temperatures. Reduction of free volume has also significant effects on gas crossover which will be discussed in Section 3.6.

3.4. Proton conductivity

The proton conductivity values of the composite membranes are listed in the Table 4. All measurements were conducted under ambient conditions with temperature of 23 °C and relative humidity (RH%) of 30 ± 5%. For comparison, the proton conductivity of pure Nafion is also shown in this table. It can be seen from Table 4 that the highest value of proton conductivity is obtained by pure Nafion and thus impregnation of silica into the Nafion matrix slightly decreases this conductivity value. Also, it is found from this table that the proton conductivity of the composite membranes has been decreased with increasing of the silica content of the impregnated Nafion membranes. The proton migration in Nafion-based membranes occurs primarily by Grotthuss and Vehicular mechanisms [43–45]. In Grotthuss mechanism, protons hop from the H₃O⁺ donor acid site to any neighboring acceptor water molecule, while protons transfer by the hydronium ions in vehicular mechanism. In other words, proton transfer agent in Grotthuss mechanism is immobile, whereas is mobile in vehicular mechanism. In general, water is essential for good conduction in both mechanisms. With the increasing of SiO₂ content in the membranes, the decrease in proton conductivity in spite of increase in water uptake may be attributed to a blocking effect of SiO₂ particles, which disrupt the continuity of sulfonic group clusters. The existence of these groups is responsible for the proton motion in the Grotthuss mechanism. Also, non-conducting SiO₂ particles which remain embedded in the channels connecting the clusters restrict the vehicular transport of protons [43]. Therefore, the slight decrease in proton conductivity with inorganic modification shows that the disruption of proton movement path is more significant than the water uptake increases.

3.5. Hydrogen crossover

Hydrogen crossover is an undesirable diffusion of hydrogen from the anode to the cathode through the membrane. The hydrogen which crosses over to the cathode side can directly react with oxygen at the cathode surface, resulting in fuel consumption without generation of electrical energy. Thus, the fuel efficiency and open circuit voltage (OCV) would be decreased. More severely, this direct reaction between H₂ and O₂ at the cathode can produce peroxide radicals, which attack not only the catalyst layer but also

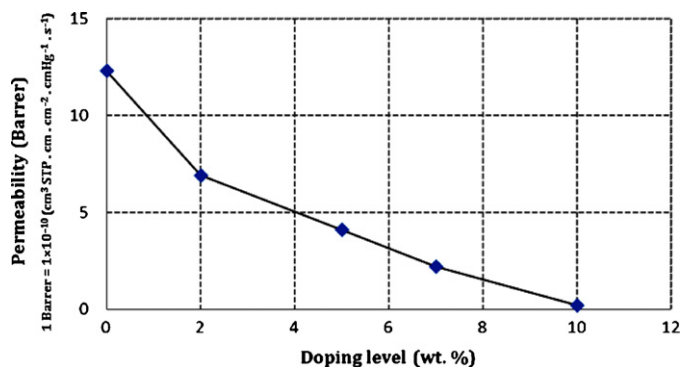


Fig. 6. Hydrogen permeability of membranes in term of Barrer.

the membrane, causing significant catalyst-layer and membrane degradation [13].

The permeability values of Hydrogen for pure Nafion and Nafion/SiO₂ composite membranes, which have been shown in Fig. 6, are listed in Table 4. According to the results, H₂ permeability of the pure Nafion membrane is reduced as SiO₂ particles are added to the membrane. Higher loading levels of doped particles lead to lower gas permeabilities.

Although the effects of incorporation of mineral particles on the Methanol permeability reduction are studied extensively [46–49], there is not any report in the literature discussing the gas permeation properties of Nafion/SiO₂ composite membranes. Felice et al. have reported recently similar trends for the reducing behavior of H₂ permeance through the Nafion/clay composite membrane [50]. They have concluded that addition of clay particles to the Nafion membrane reduces H₂ permeability.

In general, permeation mechanism for small molecules, such as H₂, is dominated by Diffusion. On the other hand, permeation of large and polar molecules, like CO₂, is controlled by Solution mechanism [51]. Reduction of the H₂ permeability by adding SiO₂ particles to the Nafion membrane could be related to the reduction of the void spaces in the membrane. In fact, mineral particles which are placed within the Nafion matrix network hinder the Hydrogen permeation by increasing tortuosities of the diffusion path. A comprehensive investigation on gas cross over of Nafion composite membrane is our current study in our laboratory.

3.6. Fuel cell performance

Polarization curves for membrane electrode assemblies containing Nafion 117 (PN), Nafion/silica membrane with 2 wt.% of SiO₂ content (NS.1), and Nafion/silica membrane with 5 wt.% of SiO₂ content (NS.2) were measured at two different temperatures and relative humidities. Each data set represents a typical steady state voltage that was taken. Fig. 7 shows the polarization curves of pure Nafion membrane and composite membranes at 70 °C and 100% RH. As seen in this Figure, at this condition, pure Nafion membrane has a better performance than the composites ones. The polarization curve of this membrane electrode assembly (PN) is located upper than SN.1 and SN.2 samples. For instance, a current density of PN was recorded as 830 mA cm⁻² against 620 mA cm⁻² for NS.1 at 0.4 V.

In fact, better performance of pure Nafion was expected according to the results of proton conduction measurements indicating its highest proton conductivity.

Furthermore, at 70 °C and 100% RH, the humidification issue (dehydration) is not a vital problem and membrane still has sufficient water for proton conduction. Polarization curves of PN, NS.1, and NS.2 samples at 110 °C and 30% RH are shown in Fig. 8. At this temperature, pure Nafion shows very poor performance while the

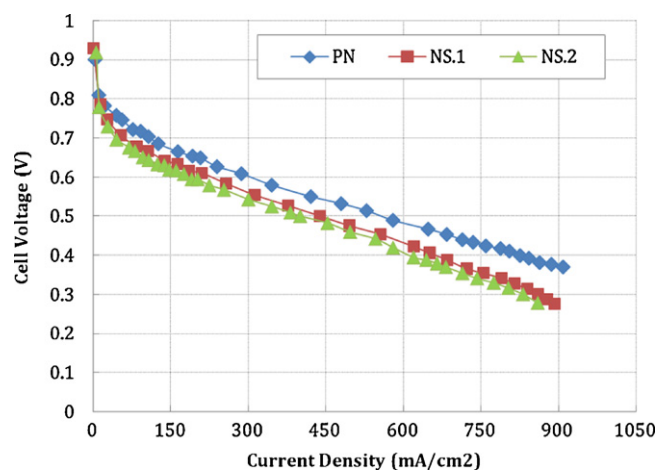


Fig. 7. PEM fuel cell performance of membranes at 70 °C and 100% relative humidity.

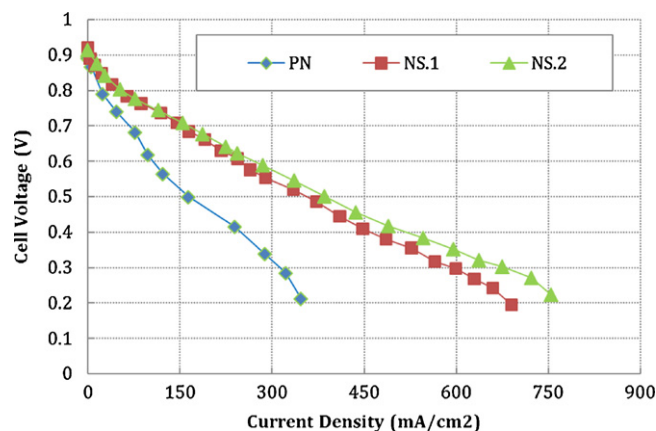


Fig. 8. PEM fuel cell performance of membranes at 110 °C and 30% relative humidity.

polarization curves of composite membranes are continued, and current density of these composite membranes is reached to about 450 mA cm⁻² at 0.4 V. Performance deterioration of pure Nafion at this condition may be explained by two reasons. The first is related to the thermal stability of Nafion. Considering the T_g of pure Nafion as 99 °C, which was measured by DSC, increasing the temperature up to T_g leads to the increasing of the membrane shrinkage, and thus its performance dramatically decreases. The second reason refers to the humidification of the membrane. At 110 °C, pure Nafion loses its water, and its resistance increases. Higher performance of NS.1 and NS.2 shows that silica particles enhance the water uptake of composite membranes, and membranes would be able to operate at elevated temperatures. Higher OCV of composite membranes compared to the pure one is another subject that could be seen from these curves. This confirms the results of hydrogen permeation measurements.

4. Conclusion

To improve the high temperature performance of PEM fuel cells, SiO₂ particles were incorporated into Nafion by sol gel technique. A 2ⁿ full factorial design of experiment was applied to optimize the sol gel reaction conditions. DOE results revealed that the optimum reaction conditions for minimizing leaching of the particles are approached according to the A3 experiment conditions. Statistical analysis of DOE has indicated that the swelling of membrane before reaction is the most dominant factor in leaching study. To reach the optimum water uptake and cell performance values,

composite membranes were made at different doping levels (2, 5, 7, 10, and 12 wt.%). Among the doped membranes, the sample with 5–8 wt.% of SiO₂ content exhibits higher water uptake. DSC results showed that incorporation of inorganic silica into the Nafion matrix increases T_g of all samples which is essential for operation of PEM fuel cells at elevated temperatures. Although proton conduction of Nafion/SiO₂ hybrid membranes with 2 and 5 wt.% of doping amount decrease slightly at ambient temperature and humidity, they show better cell performance at 110 °C and 30% RH. Moreover, doping reduced the hydrogen crossover through the membranes, leading to higher OCV values compared to bear ones.

Acknowledgment

We gratefully acknowledge the financial support for this work provided by Fuel cell Steering Committee of the Organization of Renewable Energy of Iran (SUNA) and the Iran National Science Foundation (INSF).

References

- [1] L. L. Xianguo, Principles of Fuel Cells, Taylor & Francis Group, 2006.
- [2] R. O'Hayre, Fuel Cell Fundamentals, John Wiley & Sons, Inc., 2005.
- [3] J. Larminie, J.A. Dicks, Fuel Cell Systems Explained, John Wiley & Sons, Inc., 2000.
- [4] F. Barbir, T. Fomez, International Journal of Hydrogen Energy 21 (1996) 891–901.
- [5] C. Yang, B. Costamagna, Journal of Power Sources 103 (2001) 1–9.
- [6] V. Neburchilov, J. Martin, H. Wang, Journal of Power Sources 169 (2007) 221–238.
- [7] J. Zhang, Y. Tang, Electrochimica Acta 52 (2007) 5095–5101.
- [8] S. Renaud, B. Ameduri, Progress in Polymer Science 30 (2005) 644–687.
- [9] X. Shao, G. Yin, Z. Wang, Y. Gao, Journal of Power Sources 167 (2007) 235–242.
- [10] P.L. Shao, K. Mauritz, Journal of Polymer Science Part B: Polymer Physics 34 (1996) 873–882.
- [11] S.J. Peighambari, S. Rowshanzamir, M. Amjadi, International Journal of Hydrogen Energy 35 (2010) 9349–9384.
- [12] P. Choi, N.H. Jalani, T.M. Thampan, Journal of Polymer Science Part B: Polymer Physics 44 (2006) 2183–2200.
- [13] X. Cheng, J. Zhang, Y. Tang, C. Song, J. Shen, D. Song, J. Zhang, Journal of Power Sources 167 (2007) 25–31.
- [14] M.I. Ahmad, S.M. Zaidi, S.U. Rahman, Desalination 193 (2006) 387–397.
- [15] Y. Kim, K. Kim, Current Applied Physics 6 (2006) 612–615.
- [16] M. Rikukawa, K. Sanui, Progress in Polymer Science 25 (2000) 1463–1502.
- [17] C.S. Karthikeyan, S.P. Nunes, L.A. Prado, M.L. Ponce, H. Silva, B. Ruffmann, K. Schulte, Journal of Membrane Science 254 (2005) 139–146.
- [18] G.B. Jung, F.B. Weng, A. Su, J.S. Wang, T.L. Yu, L. Lin, T.F. Yang, S. Chan, International Journal of Hydrogen Energy 33 (2008) 2413–2417.
- [19] I. Honma, H. Nakajima, O. Nishikawa, T. Sugimoto, S. Nomura, Solid State Ionics 162–163 (2003) 237–245.
- [20] L. Krishnan, Ph.D. Thesis, Univ. Princeton, 2005.
- [21] V. Singaram, J.K. Hyoung, Y.L. Sang, Journal of Power Sources 167 (2007) 325–329.
- [22] K.T. Adjemian, S. Srinivasan, J. Benziger, A.B. Bocarsly, Journal of Power Sources 109 (2002) 356–364.
- [23] K.T. Adjemian, R. Dominey, L. Krishnan, H. Ota, P. Majsztzik, T. Zhang, J. Mann, B. Kirby, L. Gatto, M. Velo-Simpson, J. Leahy, S. Srinivasan, J.B. Benziger, A.B. Bocarsly, Chemistry of Materials 18 (2006) 2238–2248.
- [24] Y. Patil, K.A. Mauritz, Journal of Applied Polymer Science 113 (2009) 3269–3278.
- [25] M. Amjadi, S. Rowshanzamir, S.J. Peighambari, M.G. Hosseini, M.H. Eikani, International Journal of Hydrogen Energy 35 (2010) 9252–9260.
- [26] E.I. Santiago, R.A. Isidoro, M.A. Dresch, B.R. Matos, M. Linardi, F.C. Fonseca, Electrochimica Acta 54 (2009) 4111–4117.
- [27] Y. Daiko, L.C. Klein, T. Kasuga, M. Nogami, Journal of Membrane Science 281 (2006) 619–627.
- [28] R. Jiang, H.R. Kunz, J.M. Fenton, Journal of Membrane Science 272 (2006) 116–124.
- [29] S. Malhotra, R. Datta, Journal of the Electrochemical Society 144 (1997) L23–L26.
- [30] K.A. Mauritz, J.D. Stefanithis, S.V. Devis, R.W. Scheetz, R.K. Pope, G.L. Wilkes, H.H. Haung, Journal of Applied Polymer Science 55 (1995) 181–190.
- [31] P. Shao, K.A. Mauritz, R.B. Moore, Chemistry of Materials 7 (1995) 192–200.
- [32] N. Miyake, J.S. Wainright, R.F. Savinell, Journal of the Electrochemical Society 148 (2001) A898–A909.
- [33] D.H. Jung, S.Y. Cho, D.H. Peck, D.R. Shin, J.S. Kim, Journal of Power Sources 106 (2002) 173–177.
- [34] H. Hagihara, H. Uchida, M. Watanabe, Electrochimica Acta 51 (2006) 3979–3985.
- [35] M. Amirinejad, S. Rowshanzamir, M.H. Eikani, Journal of Power Sources 161 (2006) 872–891.
- [36] Y. Daiko, L.C. Klein, M. Nogami, Materials Research Society Symposium Proceedings 822 (2004) 841–846.
- [37] N.H. Jalani, P. Choi, R. Datta, Journal of Membrane Science 254 (2005) 31–38.
- [38] P. Choi, N.H. Jalani, R. Datta, Journal of the Electrochemical Society 152 (2005) E84.
- [39] P. Choi, N.H. Jalani, R. Datta, Journal of the Electrochemical Society 152 (2005) E123.
- [40] T.A. Zawodzinski, L.O. Sillerud, S. Gottesfeld, Journal of Physical Chemistry 95 (1991) 6040.
- [41] Y. Kawano, Y. Wang, R.A. Palmer, S.R. Aubuchon, Polímeros 12 (2002) 96.
- [42] S.J. Peighambari, B. Pourabbas, Journal of Applied Polymer Science 106 (2007) 697–705.
- [43] M. Eikerling, A.A. Kornyshev, A.M. Kuznetsov, J. Ulstrup, S. Walbran, Journal of Physical Chemistry B 105 (2001) 3646–3662.
- [44] Z.G. Shao, P. Joghee, I.M. Hsing, Journal of Membrane Science 229 (2004) 43–51.
- [45] M.K. Mistry, N.R. Choudhury, N.K. Dutta, R. Knott, Z. Shi, S. Holdcroft, Chemistry of Materials 20 (2008) 6857–6870.
- [46] H. Kim, H. Chang, Journal of Membrane Science 288 (2007) 188–194.
- [47] W. Lee, H. Kim, T.K. Kim, H. Chang, Journal of Membrane Science 292 (2007) 29–34.
- [48] B.A. Holmberg, X. Wang, Y. Yan, Journal of Membrane Science 320 (2008) 86–92.
- [49] I.M. Krivobokov, E.N. Gribov, A.G. Okunev, G. Spoto, V.N. Parmon, Solid State Ionics 18 (2010) 1694–1701.
- [50] C. Felice, S. Ye, D. Qu, Industrial & Engineering Chemistry Research 49 (2010) 1514–1519.
- [51] A.L. Neves, I.M. Coelho, J.G. Crespo, Journal of Membrane Science 360 (2010) 363–370.